



## Climate drying and associated forest decline in the lowlands of northern Guatemala during the late Holocene

Andreas D. Mueller<sup>a,\*</sup>, Gerald A. Islebe<sup>b</sup>, Michael B. Hillesheim<sup>c,d</sup>, Dustin A. Grzesik<sup>c,d</sup>, Flavio S. Anselmetti<sup>e</sup>, Daniel Ariztegui<sup>f</sup>, Mark Brenner<sup>c,d</sup>, Jason H. Curtis<sup>c,d</sup>, David A. Hodell<sup>c,d,g</sup>, Kathryn A. Venz<sup>c,d</sup>

<sup>a</sup> Geological Institute, Department of Earth Science, ETH Zurich, Switzerland

<sup>b</sup> El Colegio de la Frontera Sur, Unidad Chetumal Herbario, AP 424, Quintana Roo, Mexico

<sup>c</sup> Department of Geological Sciences, University of Florida, Gainesville, 32611, USA

<sup>d</sup> Land Use and Environmental Change Institute (LUECI), University of Florida, Gainesville, 32611, USA

<sup>e</sup> Eawag, Swiss Federal Institute of Aquatic Science and Technology, Dübendorf, Switzerland

<sup>f</sup> Section of Earth Sciences, University of Geneva, Geneva, Switzerland

<sup>g</sup> Department of Earth Sciences, University of Cambridge, Cambridge, CB2 3EQ, UK

### ARTICLE INFO

#### Article history:

Received 29 February 2008

Available online 29 November 2008

#### Keywords:

Guatemala

Holocene

Lake sediments

Environmental changes

Tropical palaeoclimate

### ABSTRACT

Palynological studies document forest disappearance during the late Holocene in the tropical Maya lowlands of northern Guatemala. The question remains as to whether this vegetation change was driven exclusively by anthropogenic deforestation, as previously suggested, or whether it was partly attributable to climate changes. We report multiple palaeoclimate and palaeoenvironment proxies (pollen, geochemical, sedimentological) from sediment cores collected in Lake Petén Itzá, northern Guatemala. Our data indicate that the earliest phase of late Holocene tropical forest reduction in this area started at ~4500 cal yr BP, simultaneous with the onset of a circum-Caribbean drying trend that lasted for ~1500 yr. This forest decline preceded the appearance of anthropogenically associated *Zea mays* pollen. We conclude that vegetation changes in Petén during the period from ~4500 to ~3000 cal yr BP were largely a consequence of dry climate conditions. Furthermore, palaeoclimate data from low latitudes in North Africa point to teleconnective linkages of this drying trend on both sides of the Atlantic Ocean.

© 2008 University of Washington. All rights reserved.

### Introduction

Late Holocene tropical forest reduction in the Maya lowlands of northern Guatemala has been documented in palaeoenvironmental studies that investigated pollen records in lacustrine sediment archives (Vaughan et al., 1985; Islebe et al., 1996; Leyden, 2002). This vegetation change was generally interpreted as being exclusively a consequence of ancient Maya activities (e.g. forest clearance, slash and burn agriculture) (Deevey et al. 1979; Binford 1983; Vaughan et al. 1985; Brenner 1994). In some cases, however, it was not possible to distinguish the relative significance of human- versus climate-induced vegetation change (Islebe et al., 1996; Curtis et al., 1998). The question remains, whether the forest decline was driven solely by anthropogenic deforestation or whether it was partly attributable to climate changes (Hodell et al., 2000; Brenner et al., 2002). Here we

address this issue and present multiple palaeoclimate and palaeoenvironment proxies (pollen, geochemistry, sedimentology) from sediment cores collected in Lake Petén Itzá in Petén, northern Guatemala (Fig. 1).

Lake Petén Itzá is a closed basin, so that its water level varies in response to the changing ratio between evaporation and precipitation (E/P) (Curtis et al., 1998; Hillesheim et al., 2005b; Anselmetti et al., 2006; Hodell et al., 2008). Its sediment record preserves an archive of past climate changes and is an ideal repository of information to investigate the complex interactions among climate, environment and ancient Maya culture during the Holocene. In this study, we focus on the time window from ~8000 to ~1000 cal yr BP to study the palynologically documented middle to late Holocene tropical forest decline in the Petén. In particular, we investigate the relation between vegetation changes and climate changes during the late Holocene in this lowland tropical area. To assess the regional or even extra-regional scale of our findings from Lake Petén Itzá, we compare them with palaeoclimate data from other sites in the circum-Caribbean region. We also discuss the potential role of the changing mean position of the Atlantic

\* Corresponding author. Geological Institute, ETH Zurich, Universitaetstrasse 16, 8092 Zurich, Switzerland.

E-mail address: [andreas.mueller@erdw.ethz.ch](mailto:andreas.mueller@erdw.ethz.ch) (A.D. Mueller).

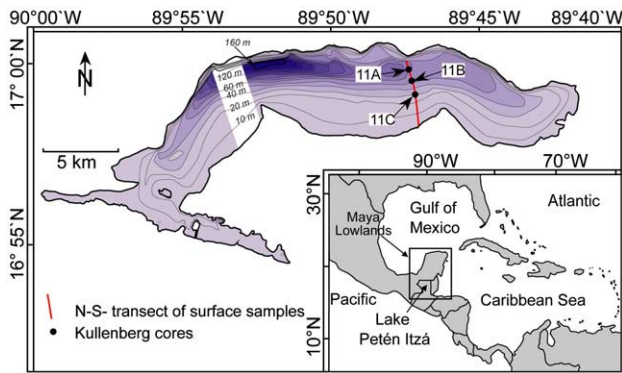


**Figure 1.** Bathymetric map of Lake Petén Itzá showing the locations of Kullenberg cores 11A, 11B, 11C collected in 2002 and showing the north–south water–depth transect of surface sediments collected in 2006 (red line). Numbers in italics are water depths in meters (depth contours = 10 m). Inset shows the location of Lake Petén Itzá in northern Guatemala.

Intertropical Convergence Zone (ITCZ) as a driving mechanism for the observed climate change.

### Study site

Lake Petén Itzá (17°00'N, 89°55'W) is the deepest lake (maximum water depth [wd] ~160 m) in the lowlands of Central America. It is located in the Department of Petén, in the Maya lowlands of northern Guatemala (Fig. 1). Lake Petén Itzá is composed of two connected basins. The deeper, northern basin occupies a large half-graben formed by a series of east–west-aligned *en-echelon* faults (Vinson, 1962), whereas the smaller southern basin is much shallower, averaging only ~5 m in water depth. Presently, the water of Lake Petén Itzá is dilute (11.22 meq/l) and dominated by calcium and bicarbonate, with magnesium and sulfate following closely in concentration (Hillesheim et al., 2005b). Lake water pH is high (~8.0) and is saturated with respect to calcium carbonate. Thermal stratification persists in the lake throughout most of the year, with hypolimnetic temperatures averaging ~25.4°C, close to the mean annual air temperature.

Lake Petén Itzá is situated in a climatically sensitive region where the amount of rainfall is related to the seasonal migration of the ITCZ and the Azores–Bermuda high-pressure system (Hastenrath, 1984). Heavy rains between June and October are associated with the northward migration of the ITCZ and the Azores–Bermuda high-pressure system. This period is characterized by weak trade winds and warm sea surface temperatures in the Atlantic between about 10° and 20°N. The rainy season is followed by a pronounced dry season during the winter (January to May) as the ITCZ and the Azores–Bermuda high move equatorward (i.e. southward) and strong trade winds become predominant in the Caribbean Sea region and in the Gulf of Mexico.

### Materials and methods

In June 2002, we retrieved six piston sediment cores from Lake Petén Itzá along a north–south water depth transect from 9.7 to 63.2 m using a Kullenberg-type piston corer (Hillesheim et al., 2005b; Anselmetti et al., 2006). This study focuses primarily on cores PI 8-VI-02 11A (water depth ~60 m), PI 5-VI-02 11B (water depth ~52 m), and PI 9-VI-02 11C (water depth ~30 m), hereafter referred to as cores 11A, 11B, and 11C (Fig. 1). Age control for cores 11A, 11B, and 11C is based on 19 accelerator mass spectrometry (AMS) C-14 dates on terrestrial organic matter (wood, leaf, or charcoal) (Table 1). Fifteen ages were published by Hillesheim et al. (2005b) and four additional ages were obtained for this study. For inter-core correlation between measured C-14 ages of cores 11C, 11B, and 11A, a stratigraphic framework was established by correlating sedimentologic features among the cores

(Fig. 2). This correlation enables the use of all radiocarbon dates to produce a detailed age–depth model of the three cores (Fig. 3). In January 2006, we used a clamshell dredge to collect surface sediment samples along the same north–south water–depth transect where Kullenberg cores were retrieved in 2002 (Fig. 1).

Past changes in the ratio of E/P were reconstructed using a geochemical proxy (elemental geochemistry, stable oxygen isotope geochemistry) applied to down-core and surface sediments. Inorganic carbon (IC) was determined by coulometric titration using a UIC/Coulometrics 5011 coulometer coupled with a UIC 5240-TIC carbonate autosampler. Weight percent calcium carbonate (CaCO<sub>3</sub>%) was calculated by multiplying IC by 8.33. Total weight percent carbon (TC) was measured using a Carlo Erba NA 1500 CNS elemental analyzer with autosampler. Weight percent organic carbon (OC) was estimated by subtracting IC from TC, weight percent organic matter (OM%) was estimated by multiplying OC by 2.2, and weight percent inorganic clay was estimated by subtracting the sum of CaCO<sub>3</sub> and OM from 100%. Oxygen isotopic ratios in the sediment of core 11C were measured on gastropod shells (*Cochliopina* sp.). Sediment samples were disaggregated in 3% H<sub>2</sub>O<sub>2</sub> and washed through a 63-μm sieve. Coarse material (>63 μm) was dried at 60°C. Gastropod shells were picked from the dried samples, soaked in 15% H<sub>2</sub>O<sub>2</sub>, cleaned ultrasonically in deionized water, and rinsed with methanol before drying. Approximately 15 gastropod shells were used to constitute a sample, which was ground to a fine powder. A fraction of this powder was analyzed from each sample. Samples were reacted in 100% orthophosphoric acid at 90°C using a ThermoFinnigan Kiel III automated preparation system. Isotopic ratios of purified CO<sub>2</sub> gas were measured online with a ThermoFinnigan-MAT 252 mass spectrometer. All isotopic values are reported in standard delta (δ) notation relative to the VPDB standard. Relative elemental concentrations in the sediments of core 11B were measured at high resolution (2 mm), using an Avaatech X-ray fluorescence (XRF) core-scanner at the University of Bremen (Hillesheim et al., 2005a). Core 11B was scanned at 10 kV when amperage was set at 1.0 mA.

Past vegetation changes in the watershed of Lake Petén Itzá were inferred using shifts in fossil pollen assemblages and changes in the carbon isotope signature (δ<sup>13</sup>C) of terrestrially derived, long-chain *n*-alkanes (C31 and C33) in the sediment record. Samples for pollen analysis were processed using 1–2 cm<sup>3</sup> of sediment taken from core 11C at 3-cm intervals. Pollen samples were prepared with standard laboratory procedures, i.e. KOH, HCl and acetolysis. Exotic *Lycopodium* spores were added to every sample before chemical processing. All residues were mounted in glycerine jelly. Pollen taxa were identified using Roubik and Moreno (1991), and the reference collection of the Ecosur Herbarium. A pollen sum of 200, excluding aquatic taxa, ferns and fungal spores, was targeted. Some samples had pollen of few taxa. Taxa were grouped by ecological preference: tropical forest, pine and temperate taxa, and disturbance taxa. Alkane extraction and isolation methods followed the procedures of Newell (2005). Lipids were extracted from 3–5 g of dry sediment using 2:1 methylene chloride/methanol in a Dionex Accelerated Solvent Extractor 300. After solvent exchange, samples were eluted through a 1 cm×29 cm glass column filled with 2.5 g of 5% deactivated silica gel to separate the non *n*-alkane fraction. Samples were urea adducted to obtain straight chain *n*-alkanes. Purity and concentration were checked with a Perkin Elmer 8500 Gas Chromatograph (GC). The dilutions for GC–IRMS analysis were calculated and samples were transferred to glass autosampler vials. Carbon isotopic analyses were performed using an Agilent 6890 GC connected to a Thermo Finnigan Delta+XL Mass Spectrometer via a GC–C III interface.

### Proxy indicators of environmental changes

To reconstruct past changes in the ratio of E/P, we use a geochemical proxy. We assume that lower rainfall (higher E/P)

**Table 1**

Accelerator mass spectrometry (AMS) radiocarbon dates and calibrated ages of terrestrial organic matter for samples from Lake Petén Itzá cores PI 8-VI-02 11A (11A), PI 5-VI-02 11B (11B) and PI 9-VI-02 11C (11C)

Core	Accession number	Material	Depth in core (cm)	Depth (blf) <sup>a</sup> (cm)	$\delta^{13}\text{C}$ (‰)	Radiocarbon age (1 $\sigma$ , <sup>14</sup> C yr BP)	Calibrated age <sup>b</sup> (1 $\sigma$ , cal yr BP)	Projected depth (blf) <sup>a</sup> to core 11A, 11B, and/or 11C (cm)
PI 8-VI-02 11A	CAMS 99102 <sup>c</sup>	Leaf	18.0	76.0	-23.31	1660±40	1605±85	-
11A	CAMS 99103 <sup>c</sup>	Wood	132.0	190.0	#	2095±35	2060±60	169.0 (core 11B)
11A	CAMS 101228 <sup>c</sup>	Wood	190.0	248.0	#	2530±60	2620±130	216.0 (core 11B)
11A	CAMS 99104 <sup>c</sup>	Wood	240.0	298.0	-22.27	2570±45	2650±110	245.0 (core 11B) 58.0 (core 11C)
11A	CAMS 92837 <sup>c</sup>	Wood	296.0	354.0	-30.30	3240±30	3440±40	284.0 (core 11B)
11A	CAMS 99105 <sup>c</sup>	Wood	312.0	370.0	-31.68	3525±25	3785±65	308.0 (core 11B)
11A	CAMS 101230 <sup>c</sup>	Leaf	390.0	448.0	#	6155±50	7075±85	384.0 (core 11B)
11A	CAMS 99106 <sup>c</sup>	Wood	406.0	464.0	#	6585±35	7470±35	425.0 (core 11B)
11A	CAMS 92836 <sup>c</sup>	Wood	432.0	490.0	-30.80	7925±30	8785±145	456.0 (core 11B)
11A	CAMS 101231 <sup>c</sup>	Wood	448.0	506.0	-28.67	8425±30	9460±25	474.0 (core 11B)
11A	CAMS 101232 <sup>c</sup>	Wood	489.0	547.0	#	9470±110	10820±250	519.0 (core 11B)
11A	CAMS 101233 <sup>c</sup>	Wood	494.0	552.0	-22.70	9555±30	10915±155	-
PI 5-VI-02 11B	CAMS 94606 <sup>c</sup>	Charcoal	342.0	365.0	-27.12	5930±40	6735±65	445.0 (core 11A)
11B	CAMS 92835 <sup>c</sup>	Wood	410.0	433.0	-28.30	7330±40	8115±75	470.0 (core 11A)
PI 9-VI-02 11C	CAMS 115792	Wood	43.0	68.0	#	3235±40	3470±80	-
11C	ETH 33385	Wood	50.0	75.0	-33.00	4055±55	4525±95	-
11C	ETH 33386	Wood	78.0	103.0	-26.80	7515±65	8305±95	-
11C	CAMS 115793	Wood	94.0	119.0	#	8520±60	9510±30	-
11C	CAMS 94607 <sup>c</sup>	Charcoal	140.0	165.0	-15.67	9665±45	11030±160	-

Radiocarbon ages were measured at the Center for Accelerator Mass Spectrometry (CAMS) at Lawrence Livermore National Laboratory, and at the AMS Facilities ETH/PSI, Zurich. All radiocarbon dates were converted to calendar years with the program OxCal version 3.10 (Bronk Ramsey, 2005) using atmospheric data from Reimer et al. (2004). All radiocarbon ages were corrected to  $\delta^{13}\text{C}$  values of -25‰ using stable isotope measurements. Samples indicated with # were too small for  $\delta^{13}\text{C}$  analysis and were assumed to be -25‰.

<sup>a</sup> Depth below lake floor (blf).

<sup>b</sup> Calibrated ages are reported in cal yr BP (before 1950).

<sup>c</sup> Radiocarbon ages, which have been published by Hillesheim et al. (2005b) but recalibrated for this study with OxCal version 3.10 (Bronk Ramsey, 2005).

reduces the delivery of detrital elements Ti, Fe and Al to the lake. Higher E/P also concentrates dissolved substances in the water column, thereby causing increased precipitation of authigenic carbo-

nate (CaCO<sub>3</sub>). Thus, we inferred past changes in E/P from the shifting ratio of Ca/ $\Sigma$ (Ti, Fe, Al) in the sediment record. Higher ratios reflect dry conditions and lower ratios reflect wet conditions. We also

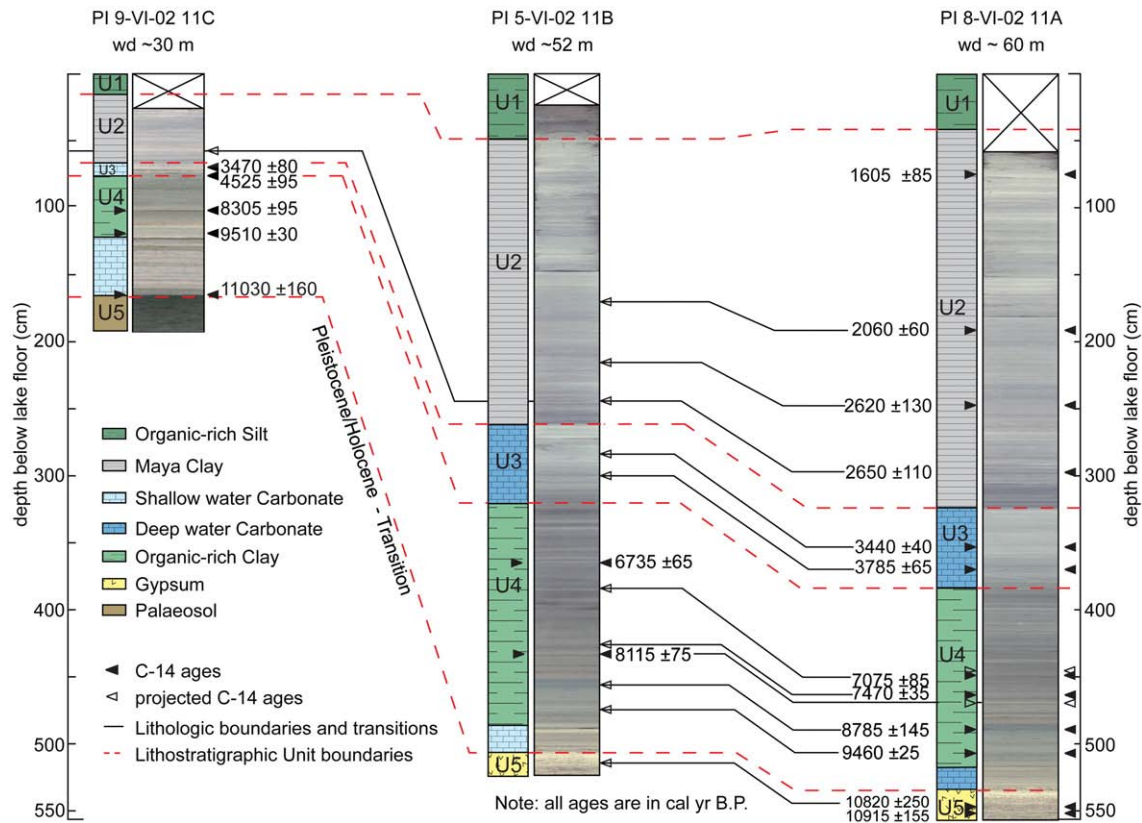


**Figure 2.** Photographic images and schematic divisions of lithologic and lithostratigraphic Units of Kullenberg cores PI 9-VI-02 11C, PI 5-VI-02 11B, and PI 8-VI-02 11A collected in Lake Petén Itzá (Hillesheim et al., 2005b). Correlation of sedimentologic features and C-14 ages among cores is indicated by black solid lines. Boundaries of lithostratigraphic Units are shown by red dashed lines. Missing uppermost sections in core 11B, and 11C are indicated at the top of the photographic image.

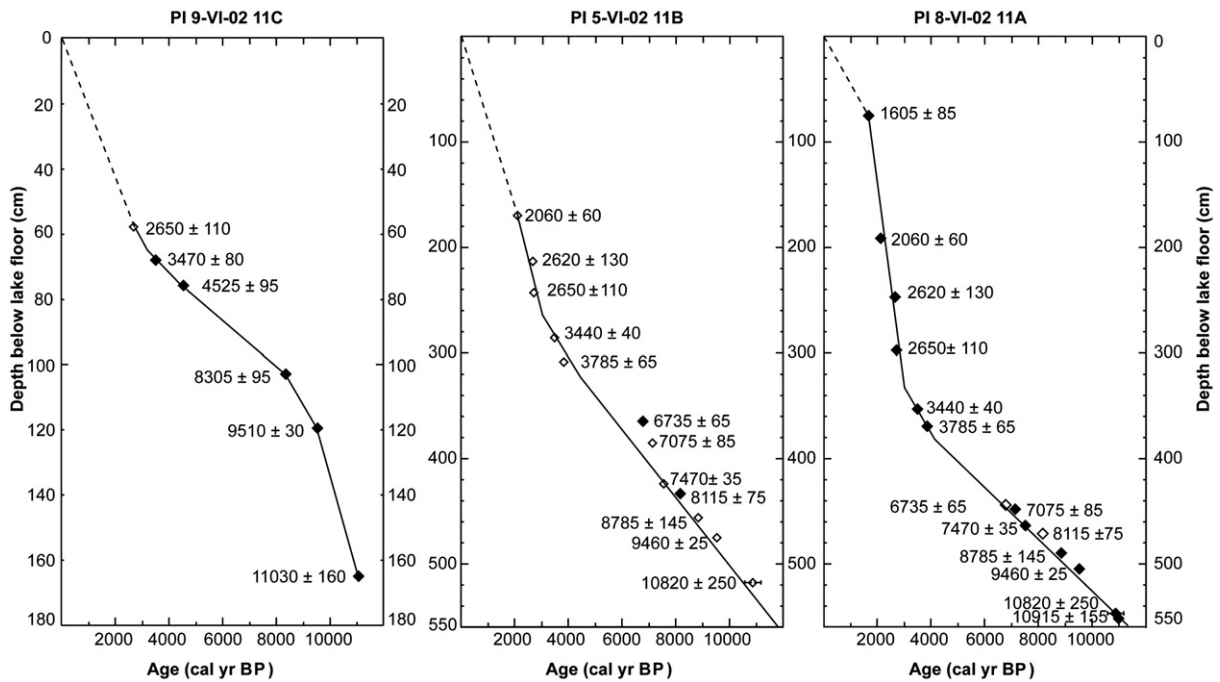


**Figure 3.** Calibrated ages (cal yr BP) of samples of terrestrial organic matter versus depth below lake floor for Lake Petén Itzá cores 11A, 11B and 11C. The core chronology was established by linear interpolation between AMS C-14 dates (open diamonds  $\diamond$  represent projected ages, see Figure 2). Dating error on all samples is smaller than the plot symbols, except where indicated by an error bar.

explored past changes in E/P by measuring stratigraphic variations in the oxygen isotope composition ( $\delta^{18}\text{O}$ ) of gastropod shells. Lower values reflect moister conditions and greater values reflect drier

conditions (Hodell et al., 1991). In addition, past changes in the water level of Lake Petén Itzá (i.e., shifts in E/P) were inferred by first establishing modern relationships between surface sediment

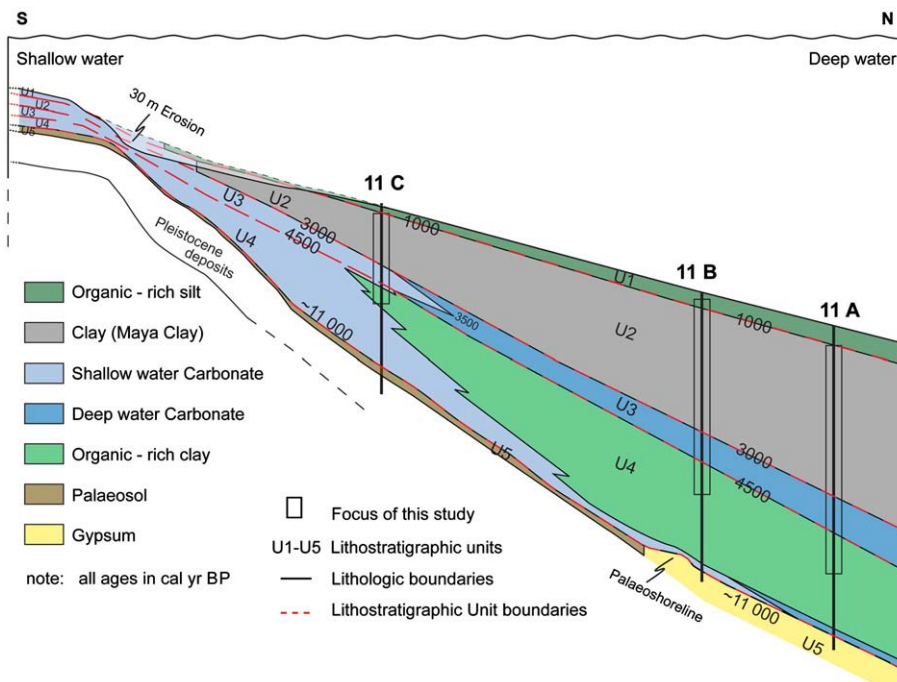


**Figure 4.** Schematic diagram of the stratigraphic sequence architecture of Holocene Lake Petén Itzá sediments showing the time-transgressive migration from lithologies along a south-north water depth transect with transitions from shallow-water to deep-water depositional environments. Five lithostratigraphic Units (U5 to U1) were defined, indicated by red dashed lines. The palaeoshoreline represents a lake level lowstand at the termination of the arid last glacial period in the latest Pleistocene, when lake level was ~58 m below modern lake level (Hillesheim et al., 2005b; Anselmetti et al., 2006). Note the southward migration of facies belts during the transgression and lake level rise at the base of U4 and the northward migration of the shallow water sediments in 11C in Unit U3 at ~4500 cal yr BP indicating a lake level lowering. The disappearance of uppermost lithostratigraphic units at the transition from deep-water to shallow-water environments between 30 m and 15 m water depth, and the reappearance of these lithostratigraphic units in water depths < 15 m, is interpreted to be a consequence of erosion by water circulation down to the top of the metalimnion (Anselmetti et al., 2006).

composition (% CaCO<sub>3</sub>, % organic matter OM, % clay, and gastropod content) and lake water depth, and then applying these relationships to the composition of sediments in core 11C.

Vegetation changes in the Lake Petén Itzá catchment were reconstructed from fossil pollen assemblages and from shifts in carbon isotopic ratios ( $\delta^{13}\text{C}$ ) of terrestrially derived long-chain *n*-alkanes (C31 and C33). The latter measure reflects changes in the relative abundance of C3 plants (e.g., trees and shrubs) and C4 plants (e.g., tropical grasses) in the watershed (Huang et al., 2001). Increasing  $\delta^{13}\text{C}$  values reflect a relative increase of C4 to C3 plant biomass in the watershed.

**Results**

*Lithostratigraphy and chronology*

The Holocene sediment record from Lake Petén Itzá reveals five lithostratigraphic Units (U5–U1), each of which is characterized by a lithology that is also seen in surface sediments collected along the transect from modern shallow-water to deep-water depositional environments (Fig. 4). Sediments in Unit U5 (latest Pleistocene), in the lower part of Unit U4 (early Holocene), and in Unit U1 (~1000 cal yr BP to present) fall outside our time window of interest, and are not described in detail.

Sediments of Unit U5 (late Pleistocene to ~11 000 cal yr BP) in cores 11A and 11B are characterized by autochthonous gypsum deposits (Figs. 2 and 4) (Hillesheim et al., 2005b; Anselmetti et al., 2006). The landward equivalent of Unit U5 is marked by an organic-rich paleosol in core 11C (Figs. 2 and 4). The lower part of overlying Unit U4 (~11,000 to ~8000 cal yr BP) is marked in all the cores (11A, 11B, and 11C) by carbonate-rich sediments. The upper part of Unit U4 (~8000 to ~4500 cal yr BP) in each core consists of dark green, mm-scale laminated, organic-rich clay. The CaCO<sub>3</sub> content in Unit U4 of core 11C, and the Ca/Σ (Ti, Fe, Al) ratio in core 11B display low and unchanging values (Fig. 5). Accumulation of these sediments was slow (0.03 cm/yr in 11A and 11B, and 0.01 cm/yr in 11C) (Fig. 3). The lithologic transition from U4 to overlying U3 at ~4500 cal yr BP is

expressed in core 11C by a shift from finely laminated clay to gastropod-rich (*Pyrgophorus* sp., *Cochliopina* sp., and *Tryonia* sp.) carbonate silt, and by an increase in carbonate content from 10% to 70%, which peaks at ~3500 cal yr BP (Fig. 5a). In deep-water cores 11A and 11B, this transition is marked by greater amounts of authigenic calcite crystals, expressed as an increase in the ratio of Ca/Σ (Ti, Fe, Al), which also reaches a maximum at ~3500 cal yr BP (Fig. 5b). Sedimentation rates in U3 increased to 0.06 and 0.05 cm/yr in cores 11A and 11B, respectively, and remained constant in core 11C (0.01 cm/yr). Sediment of Unit U2 (~3000 to ~1000 cal yr BP) in all cores consists of a thick, detrital inorganic clay unit. This lithology has been identified in other Petén lakes and was designated “Maya Clay” (Deevey et al., 1979; Anselmetti et al., 2007). The sedimentation rate increased in the “Maya Clay” zone to 0.15 cm/yr in 11A, to 0.10 cm/yr in 11B, and to 0.02 cm/yr in 11C. Uppermost sediments of Lake Petén Itzá (Unit U1) are composed of organic-rich silt, often referred to as “Post-Maya gyttja” (Brenner et al., 2002). Due to the Kullenberg coring technique and the high water content of these sediments, we did not recover Unit U1 in cores 11A and 11B, and only the lower part of this Unit was collected in core 11B (Fig. 2). The oxygen isotope composition ( $\delta^{18}\text{O}$ ) of gastropod shells in core 11C displays a gradual decrease from ~2.75‰ at the bottom of Unit U4, ~8000 cal yr BP, to ~1.0‰ at the top of Unit U2, ~1300 cal yr BP (Fig. 5a).

*Pollen and  $\delta^{13}\text{C}$  isotopes*

The pollen assemblage of U4 in core 11C is dominated by tropical moist forest taxa such as *Brosimum* and other Moraceae (Figs. 5a and 6). At the transition from U4 to U3, a change from dense vegetation to a more open, savanna-like landscape is indicated by a decline in the relative abundance of tropical forest taxa and an increase in *Pinus* (pine), *Quercus* (oak), Poaceae (grasses), and secondary taxa. Remains of the alga *Botryococcus* are also abundant in U3. Sediments of U2 are characterized by an increase in pollen of disturbance taxa such as *Asteraceae*, *Ambrosia*, and *Chenopodiaceae*, and by the first appearance of *Zea mays* pollen. Carbon isotope values ( $\delta^{13}\text{C}$ ) of C31 and C33 *n*-alkanes show a gradual increase

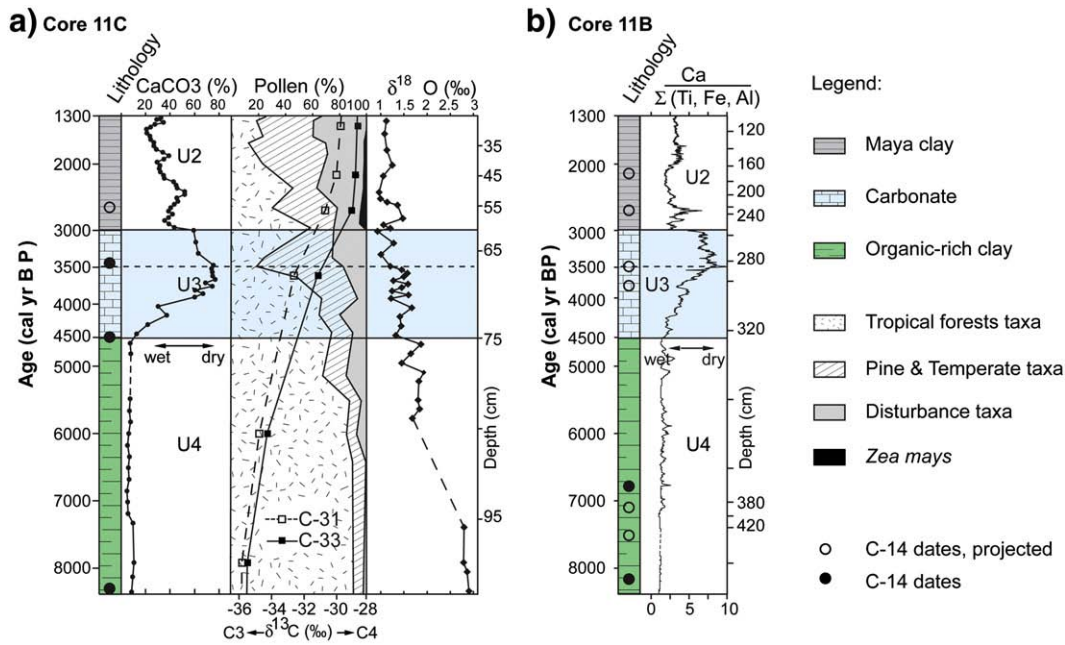


**Figure 5.** Palaeoenvironmental and palaeoclimate proxies from the late Holocene sediment record of Lake Petén Itzá versus time (cal yr BP). (a) Core PI 9-VI-02 11C (water depth ~30 m): lithology, weight percent calcium carbonate (CaCO<sub>3</sub>, %), lithostratigraphic Units U, pollen record and  $\delta^{13}\text{C}$  ratio of long-chain *n*-alkanes, and  $\delta^{18}\text{O}$  ratio of gastropods versus time (cal yr BP). (b) Core PI 5-VI-02 11B (water depth ~52 m): lithology, lithostratigraphic Unit U, and Ca/Σ (Ti, Fe, Al) ratio versus time (cal yr BP).

from the base of U4 (~36%) to the top of U2 (~28%), indicating a relative increase of C4 plant biomass in the watershed (Fig. 5a).

#### Modern sedimentology of Lake Petén Itzá

Surface sediment samples from the shoreline to a water depth of ~23 m ('shallow water zone') in Lake Petén Itzá (Fig. 7) are characterized by gastropod-rich carbonate silt, with low organic matter and clay content (>60% CaCO<sub>3</sub>; <5% OM; <20% Clay; gastropods: *Pyrgophorus* sp., *Cochliopina* sp., and *Tryonia* sp.). In contrast, surface sediments deposited in water >23 m deep ('deep water zone'), are characterized by low carbonate content, no gastropods, but high amounts of organic matter and clay (10–20% OM; >80% Clay; <10% CaCO<sub>3</sub>).

## Discussion

### Palaeoenvironmental interpretation

Gypsum of Unit U5 was deposited during a lake-level lowering of 58 m in the Late Glacial period (Hillesheim et al., 2005b; Anselmetti et al., 2006). A prominent palaeoshoreline marks the transition between the lacustrine gypsum deposits lakeward and the paleosol horizon landward, which was formed in subaerially exposed areas (Fig. 4). The subsequent lake level rise is recorded at the base of Unit U4 by carbonate-rich transgressional sediments (Fig. 4). The finely laminated, organic-rich clay of U4 (from ~8000 to ~4500 cal yr BP) and the high concentration of tropical moist forest taxa in the pollen record during this time indicate deposition in deeper water under wet climate conditions of the middle Holocene. This interpretation is consistent with the Holocene 'thermal maximum,' a wet phase observed in several other palaeoclimate records from the circum-Caribbean region (e.g. Hodell et al., 1991; Haug et al., 2001). The prominent lithologic transition in core 11C from laminated clay (U4) to the overlying gastropod-rich carbonate silt (U3) (Figs. 2 and 4) at ~4500 cal yr BP was interpreted using our surface sediment calibration data set (Fig. 7). These samples indicate that the modern shallow-water zone is composed of gastropod-rich, silty carbonates (Fig. 7) very similar to the lithology of U3 in core 11C. This similarity

suggests that the lithologic transition from U4 to U3 at Site 11C indicates a lake level lowering that reflects an increase in the ratio of E/P caused by the onset of climatic drying. The modern water depth at site 11C is ~30 m, or ~7 m deeper than the modern, maximum water depth for deposition of the shallow-water facies (i.e., <~23 m; Fig. 7). We thus conclude that a lake level lowering relative to the modern stage of at least 7 m was required to deposit shallow-water facies at the site of core 11C. Lake level lowering beginning at ~4500 cal yr BP is also inferred from the upcore increase in Ca/Σ (Ti, Fe, Al) at the U3–U4 transition in deep-water core 11B (Fig. 5b). It reflects elevated amounts of authigenic carbonates that indicate higher ion concentrations in the water, and therefore increasing E/P. Furthermore, lake level decline at this time is also registered by the high concentrations of *Botryococcus* in U3 of core 11C (Fig. 6), which indicate an algal response to lower water level and associated higher nutrient concentration in the lake water (Batten and Grenfell, 1996). The CaCO<sub>3</sub> record of core 11C and the Ca/Σ (Ti, Fe, Al) record of core 11B both suggest that the drying trend in Petén began at ~4500 cal yr BP, peaked at ~3500 cal yr BP, and terminated at ~3000 cal yr BP (Fig. 5). The oxygen isotope record from Lake Petén Itzá, however, does not record an increase in δ<sup>18</sup>O values at ~4500 cal yr BP, as might be expected with increasing E/P (Fig. 5a). We suggest that this lack of response in the oxygen isotope data may reflect low sensitivity of this climate proxy in this large-volume lake (Curtis et al., 1999). The pollen record in Unit U3 of core 11C reveals a late Holocene decline in tropical moist forest and expansion of an open, savanna-like landscape in Petén that coincided with this drying trend. The question remains as to whether this palynologically documented forest decline during the middle to late Holocene was attributable to climate changes, human disturbance, or both. The shift from the Maya Clay (U2) to the overlying organic-rich silt of U1 was interpreted previously to be the result of forest recovery after human pressure declined following the Maya Classic period (Vaughan et al., 1985; Brenner et al., 2002; Leyden, 2002).

Coincidence of water level lowering in Lake Petén Itzá with tropical forest reduction at ~4500 cal yr BP suggests that the vegetation shift in Petén was driven, at least in part, by climatic drying. This suggestion is further supported by the absence of *Zea*

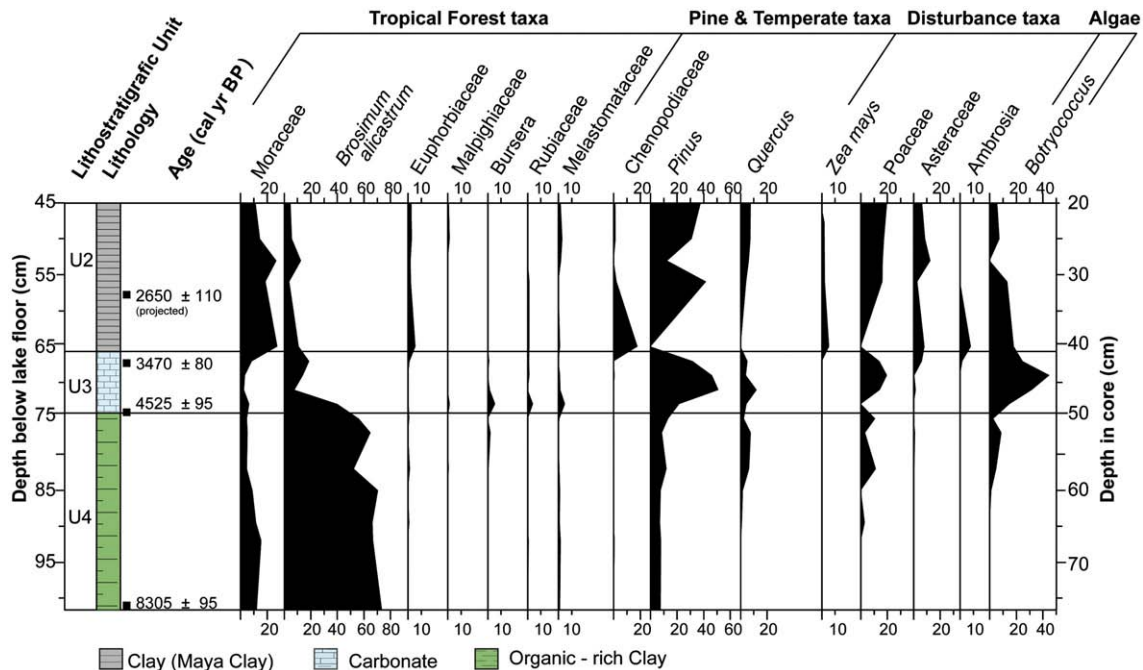


**Figure 6.** Pollen percentage diagram for Lake Petén Itzá core PI 9-VI-02 11C. Pollen taxa were grouped by ecological preference: tropical forest taxa, pine and temperate taxa, and disturbance taxa. On the left side of the diagram, lithostratigraphic Units and their corresponding lithologic composition are shown.

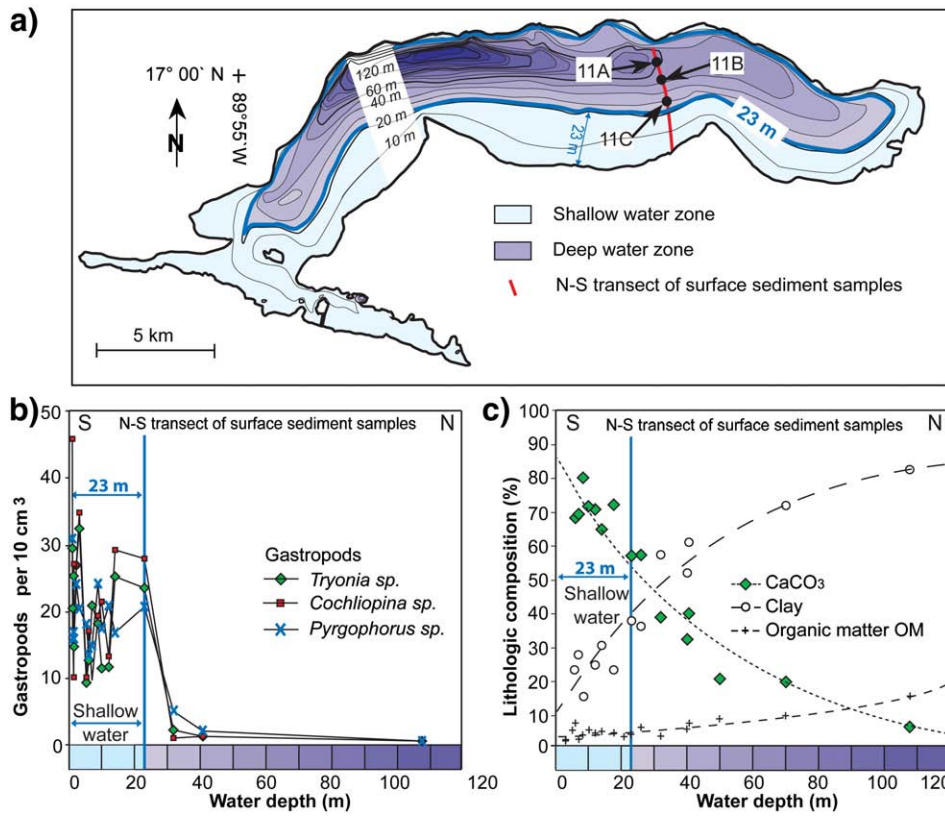


**Figure 7.** Modern composition of surface sediment samples versus water depth in Lake Petén Itzá. (a) Bathymetric map of Lake Petén Itzá (Anselmetti et al., 2006) illustrating the north–south water–depth transect of collected surface sediments (red line), and the locations of cores 11A, 11B, and 11C (black dots). The solid blue line at a water depth of 23 m indicates a transition from the modern shallow-water to modern deep-water depositional environment. (b, c) Gastropod content per 10 cm<sup>3</sup> (b), and lithologic composition (c) of surface sediment samples versus water depth along a north–south water depth transect.

*mays* pollen in Unit U3 (Fig. 6). The first *Zea mays* pollen do not appear before the deposition of the Maya Clay (Unit U2) at ~3000 cal yr BP in the record of 11C (Figs. 5a and 6) indicating that initial vegetation changes preceded substantial early Maya agricultural activity in the Petén Itzá catchment. In contrast, other studies provide the earliest evidence for *Zea mays* pollen at ~4500 cal yr BP in the Mirador Basin of northern Guatemala (Wahl et al., 2006), prior to ~5000 cal yr BP in the Pulltrouser Swamp in Belize and coastal Guatemala (Jones, 1994; Pohl et al., 1996; Neff et al., 2006), and more than ~7000 years ago in the Gulf Coast lowlands (Pope et al., 2001; Pohl et al. 2007). This pattern indicates that adoption of maize agriculture varied across the Maya lowlands and adjacent regions. Thus, the relative contributions of climate change and human land use as drivers of vegetation change in the late Holocene may have differed across the region. In some areas, Maya agricultural systems might have played an important role in initial forest decline, whereas elsewhere, significant human-induced biotic alterations related to more intensive agricultural systems may have followed climatically induced deforestation.

The palynological and sedimentological record from Lake Petén Itzá suggests that dry conditions in lowland Guatemala were partly responsible for late Holocene vegetation changes. However, if the initial spread of savanna in Petén between ~4500 and ~3000 cal yr BP was caused by dry climate conditions, simultaneous drying should also be evident in other palaeoclimate records from the circum-Caribbean. Indeed, several other circum-Caribbean palaeoclimatic records are consistent with the inferences for dry climate conditions in Petén between ~4500 and ~3000 cal yr BP that peaked at ~3500 cal yr BP. For instance, low metal concentrations (Ti, Fe) and high oxygen isotopic values in a marine record off

northern Venezuela (Cariaco, ODP Hole 1002C) are interpreted to record dry conditions at ~3500 cal yr BP (Haug et al., 2001; Tedesco and Thunell, 2003) (Fig. 8). Similarly, high oxygen isotopic values in lacustrine sediments from Lake Miragoane, Haiti (Hodell et al., 1991), and from Lake Valencia, northern Venezuela (Curtis et al., 1999) are interpreted to document dry conditions and/or less rainfall around 3500 cal yr BP. Furthermore, a drying trend around this time apparently occurred in the northern hemisphere tropics on both sides of the Atlantic Ocean (Fig. 9). Sediments from Lake Bosumtwi, Ghana indicate a major lake level decline at ~3200 cal yr BP (Russell et al., 2003) and several other lakes in the northern hemisphere African tropics display evidence of water-level low stands around this time (Fig. 9), e.g., Bahr-el-Ghazal, Chad and Lake Abhé, Ethiopia (Gasse, 2000). Temporal coincidence of dry conditions in the northern hemisphere tropics across America and Africa ~3500 cal yr BP indicates teleconnective linkages and suggests global-scale forcing. In contrast to the drying that is documented in the northern hemisphere tropics at ~3500 cal yr BP, palaeoclimate records from the southern Hemisphere in South America (e.g., Lake Titicaca, Peru; Baker et al., 2001) and in Africa (e.g., Lake Malawi, Malawi; Johnson et al., 2002) indicate increased humidity at this time (Fig. 9). This “out-of-phase” pattern is consistent with a southward migration of the mean meridional position of the Atlantic ITCZ (Hodell et al., 1991; Haug et al., 2001; Peterson and Haug, 2006) and suggests it is a potential explanation for the observed drying trend beginning ~4500 cal yr BP in the Petén. Southerly migration of the mean position of the Atlantic ITCZ is controlled by different forcing mechanisms, such as i) reduction of the Atlantic Meridional Overturning Circulation (AMOC), which decreases the cross-equatorial heat flux from the South to North Atlantic and strengthens the northeast trade winds (Timmermann et al., 2005; Cheng et al.,

2007), ii) decreasing latitudinal gradients of the sea surface temperature (SST), associated with cooling of SST in the North Atlantic (Chiang and Bitz, 2005; Peterson and Haug, 2006), iii) increasing intensity of the annual cycle in the southern hemisphere tropics, associated with the ~21,000-year precessional component of Milankovitch forcing (Hodell et al., 1991; Haug et al., 2001), iv) increasing land–sea ice cover in the Northern Hemisphere (Chiang and Bitz, 2005), v) weakening of the Caribbean Low-Level Jet (CLLJ) (Mestas-Nunez et al., 2007), vi) increased ENSO-variability in the tropical Pacific (Haug et al., 2001), vii) weakening of the Walker circulation (Stott et al., 2002), and/or viii) changes in the seasonal distribution of the North Atlantic Oscillation (NAO) (Giannini et al., 2001). Regardless of the forcing mechanisms that dominated and ultimately caused the inferred climate shifts, we note that the drying trend registered in the Petén, and more broadly in equatorial regions of the Northern Hemisphere, parallels an increased commitment to maize-based food production and the emergence of hierarchically organized societies on the Pacific and Gulf Coasts of Mexico (Clark and Blake 1994; Pope et al. 2001; Kennett et al., 2007) that later influenced similar cultural developments in the Maya lowlands (Rice, 1976; Rice and Rice, 1990; Neff et al. 2006).

## Conclusions

Our sedimentological, geochemical, and pollen data from Lake Petén Itzá provide new insights into the palynologically documented, late Holocene forest decline in the lowland Neotropics of northern Guatemala. First, the earliest phase of tropical forest reduction in Petén coincided with a water-level decline in Lake Petén Itzá (i.e. dry conditions) between ~4500 and ~3000 cal yr BP. Second, the onset of late Holocene forest reduction at ~4500 cal yr BP preceded the first

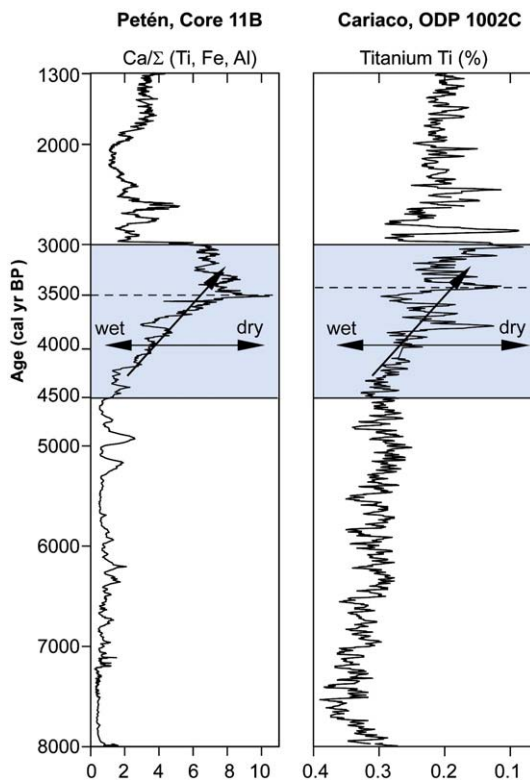


**Figure 8.** Comparison of geochemical proxies versus age in sediment cores from Lake Petén Itzá, northern Guatemala (this study) and from the marine Cariaco Basin (ODP Hole 1002C, offshore northern Venezuela; Haug et al., 2001). Both proxies are sensitive to changes in the ratio between evaporation and precipitation (E/P) and indicate a pan-Caribbean drying trend between ~4500 and ~3000 cal yr BP.

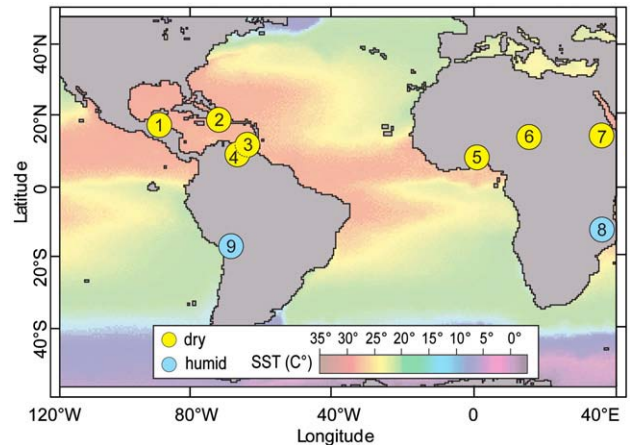


**Figure 9.** Map of sea surface temperatures (SST) (<http://atlas.snet.gob.sv>) in degrees Celsius (°C) in the Atlantic Ocean (June 1985–1997) showing sites discussed in this study. The colors represent climate conditions around 3500 cal yr BP at each site (yellow: dry, blue: humid): 1, Lake Petén Itzá, northern Guatemala (this study); 2, Lake Miragoane, Haiti (Hodell et al., 1991); 3, Cariaco Basin, offshore northern Venezuela (Haug et al., 2001); 4, Lake Valencia, Venezuela (Curtis et al., 1999); 5, Lake Bosumtwi, Ghana (Russell et al., 2003); 6, Bahr-el-Ghazal, Chad (Gasse, 2000); 7, Lake Abhé, Ethiopia (Gasse, 2000); 8, Lake Malawi, Malawi (Johnson et al., 2002); and 9, Lake Titicaca, Peru/Bolivia (Baker et al., 2001).

appearance of *Zea mays* pollen in the sediments of Lake Petén Itzá, suggesting that initial forest reduction preceded substantial agricultural activity in the watershed. Third, comparison of results from Lake Petén Itzá with other palaeoclimate data shows that forest loss in Petén coincided with a widespread drying trend. We conclude that the late Holocene vegetation change in the Maya lowlands was not associated solely with human activity, as previously suggested, but that its earliest phase was driven largely by climatic drying. Temporal correlations between climate drying, associated environmental changes in agricultural intensification and the early emergence of hierarchically organized complex societies merit further investigation by archaeologists and palaeoclimatologists.

## Acknowledgments

We thank Pru and Don Rice and an anonymous reviewer for helpful criticisms of an earlier version of this paper. We also thank M. Ploetze, D. Kennett, A. Gilli, G. Haug, and I. Hajdas for discussions and constructive comments. We are grateful to D. Schnurrenberger, D. Buck, M. Rosenmeier for help during coring operations. This work was supported by ETH Research Grant TH-1/04-1, the Swiss National Science Foundation, and the US National Science Foundation (ATM-0502030).

## References

- Anselmetti, F.S., Ariztegui, D., Brenner, M., Hodell, D.A., Rosenmeier, M.F., 2007. Quantification of soil erosion rates related to ancient Maya deforestation. *Geology* 35, 915–918.
- Anselmetti, F.S., Ariztegui, D., Hodell, D.A., Hillesheim, M.B., Brenner, M., Gilli, A., McKenzie, J.A., Mueller, A.D., 2006. Late Quaternary climate-induced lake level variations in Lake Petén Itzá, Guatemala, inferred from seismic stratigraphic analysis. *Palaeogeography Palaeoclimatology Palaeoecology* 230, 52–69.
- Baker, P.A., Seltzer, G.O., Fritz, S.C., Dunbar, R.B., Grove, M.J., Tapia, P.M., Cross, S.L., Rowe, H.D., Broda, J.P., 2001. The history of the South American tropical precipitations for the past 25,000 years. *Science* 291, 640–643.
- Batten, D.J., Grenfell, H.R., 1996. *Botryococcus*. In: Jansonius, J., McGregor, D.C. (Eds.), *Palynology: Principles and Applications*. American Association of Stratigraphic Palynologists Foundation, pp. 205–214.
- Binford, M.W., 1983. Paleolimnology of the Petén Lake District, Guatemala. *Hydrobiologia* 103, 199–203.
- Brenner, M., 1994. Lakes Salpeten and Quexil, Petén, Guatemala, Central America. In: Gierlowski-Kordesch, E., Kelts, K. (Eds.), *Global Geological Record of Lake Basins*, 1. Cambridge University Press, Cambridge, pp. 377–380.

- Brenner, M., Rosenmeier, M.F., Hodell, D.A., Curtis, J.H., 2002. Paleolimnology of the Maya lowlands: long-term perspectives on interactions among climate, environment, and humans. *Ancient Mesoamerica* 13, 141–157.
- Bronk Ramsey, C. 2005. OxCal program, Version 3.10.
- Cheng, W., Bitz, C.M., Chiang, J.C.H., 2007. Adjustment of the global climate to an abrupt slowdown of the Atlantic meridional overturning circulation. In: Schmittner, A., Chiang, J.C.H., Hemming, S.R. (Eds.), *Ocean Circulation: Mechanisms and Impacts*, 173. AGU Monograph, pp. 295–314.
- Chiang, J.C.H., Bitz, M., 2005. Influence of high latitude ice on the position of the marine intertropical convergence zone. *Climate Dynamics*, doi:10.1007/s00382-005-0040-5.
- Clark, J.E., Blake, M., 1994. Power and prestige: competitive generosity and the emergence of rank in lowland Mesoamerica. In: Brumfiel, E.M., Fox, J.W. (Eds.), *Factional Competition and Political Development in the New World*. Cambridge University Press, Cambridge, pp. 17–30.
- Curtis, J.H., Brenner, M., Hodell, D.A., Balsler, R.A., Islebe, G.A., Hooghiemstra, H., 1998. A multi-proxy study of Holocene environmental change in the Maya lowlands of Petén, Guatemala. *Journal of Paleolimnology* 19, 139–159.
- Curtis, J.H., Brenner, M., Hodell, D.A., 1999. Climate change in Lake Valencia Basin, Venezuela, ~12,600 yr BP to present. *The Holocene* 9, 609–619.
- Deevey, E.S., Rice, D.S., Rice, P.M., Vaughan, H.H., Brenner, M., Flannery, M.S., 1979. Mayan urbanism: impact on a tropical karst environment. *Science* 206, 298–306.
- Gasse, F., 2000. Hydrological changes in the African tropics since the Last Glacial Maximum. *Quaternary Science Reviews* 19, 189–211.
- Giannini, A., Kushnir, Y., Cane, M.A., 2001. Interdecadal changes in the ENSO teleconnection to the Caribbean Region and the North Atlantic Oscillation. *Journal of Climate* 14, 2867–2879.
- Hastenrath, S., 1984. Interannual variability and the annual cycle: mechanisms of circulation and climate in the tropical Atlantic sector. *Monthly Weather Review* 112, 1097–1107.
- Haug, G.H., Hughen, K.A., Sigman, D.M., Peterson, L.C., Roehl, U., 2001. Southward migration of the intertropical convergence zone through the Holocene. *Science* 293, 1304–1308.
- Hillesheim, M.B., 2005a. Climate change in Central America during the late deglacial and early Holocene inferred from lacustrine sediments in Lake Petén Itzá, Guatemala. M.S. Thesis, University of Florida, Gainesville, FL, 100 pp.
- Hillesheim, M.B., Hodell, D.A., Leyden, B.W., Brenner, M., Curtis, J.H., Anselmetti, F.S., Ariztegui, D., Buck, D.G., Guilderson, T.P., Rosenmeier, M.F., Schnurrenberger, D.W., 2005b. Climate change in lowland Central America during the late deglacial and early Holocene. *Journal of Quaternary Science* 20 (4), 363–376.
- Hodell, D.A., Brenner, M., Curtis, J.H., 2000. Climate change in the northern American tropics since the last Ice Age: implications for environment and culture. In: Lentz, D.L. (Ed.), *Imperfect Balance: Landscape Transformations in the Precolumbian Americas*. Columbia University Press, New York, pp. 13–38.
- Hodell, D.A., Curtis, J.H., Jones, G.A., Higuera-Gundy, A., Brenner, M., Binford, M.W., Dorsey, K.T., 1991. Reconstruction of Caribbean climate change over the past 10,500 years. *Nature* 352, 790–793.
- Hodell, D.A., Anselmetti, F., Ariztegui, D., Brenner, M., Bush, M.B., Correa-Metrio, A., Curtis, J.H., Escobar, J., Gilli, A., Grzesik, D.A., Guilderson, T.P., Kutterolf, S., Mueller, A.D., 2008. An 85-ka record of climate change in lowland Central America. *Quaternary Science Reviews* 27, 1152–1165.
- Huang, Y., Street-Perrott, F.A., Metcalfe, S.E., Brenner, M., Moreland, M., Freeman, K.H., 2001. Climate change as the dominant control on glacial–interglacial variations in C3 and C4 plant abundance. *Science* 293, 1647–1651.
- Islebe, G.A., Hooghiemstra, H., Brenner, M., Curtis, J.H., Hodell, D.A., 1996. A Holocene vegetation history from lowland Guatemala. *The Holocene* 6, 265–271.
- Jones, J.G., 1994. Pollen evidence for early settlement and agriculture in northern Belize. *Palynology* 18, 205–211.
- Johnson, T.C., Brown, E.T., McManus, J., Barry, S., Barker, P., Gasse, F., 2002. A high-resolution paleoclimate record spanning the past 25,000 years in southern East Africa. *Science* 296, 113–132.
- Kennett, D.J., Voorhies, B., Martorana, D., 2006. An evolutionary model for the origins of agriculture on the Pacific coast of Southern Mexico. In: Kennett, D.J., Winterhalder, B. (Eds.), *Behavioral Ecology and the Transition to Agriculture*. University of California Press, Berkeley, pp. 103–136.
- Leyden, B.W., 2002. Pollen evidence for climatic variability and cultural disturbance in the Maya lowlands. *Ancient Mesoamerica* 13, 85–101.
- Mestas-Nunez, A.M., Enfield, D.B., Zhang, C., 2007. Water vapor fluxes over the Intra-Americas Sea: seasonal and interannual variability and associations with rainfall. *Journal of Climate* 20 (9), 1910–1922.
- Newell, S. D., 2005. An Analysis of Compound Specific Carbon Isotopes of Lipid Biomarkers: A Proxy for Paleoenvironmental Change in the Maya lowlands of Peten, Guatemala. M.S. Thesis, University of Florida, Gainesville, FL, 104 pp.
- Neff, H., Pearsall, D.M., Jones, J.G., Arroyo, B., Freidel, D.E., 2006. Climate change and population history in the Pacific lowlands of southern Mesoamerica. *Quaternary Research* 65, 390–400.
- Peterson, L.C., Haug, G.H., 2006. Variability in the mean latitude of the Atlantic intertropical convergence zone as recorded by riverine input of sediments to the Cariaco Basin (Venezuela). *Palaeogeography Palaeoclimatology Palaeoecology* 234, 97–113.
- Pohl, M.E.D., Pope, K.O., Jones, J.G., Jacob, J.S., Piperno, D.R., deFrance, S.D., Lentz, D.L., Gifford, J.A., Danforth, M.E., Jossenand, J.K., 1996. Early agriculture in the Maya lowlands. *Latin American Antiquity* 7, 355–372.
- Pohl, M.E.D., Piperno, D.R., Pope, K.O., Jones, J.G., 2007. Microfossil evidence for pre-Columbian maize dispersals in the neotropics from San Andrés. *Proc Natl Acad Sci USA* 104, 6870–6875.
- Pope, K.O., Pohl, M.E.D., Jones, J.G., Lentz, D.L., von Nagy, C., Vega, F.J., Quitmyer, I.R., 2001. Origin and environmental setting of ancient agriculture in the lowlands of Mesoamerica. *Science* 292, 1370–1373.
- Reimer, P.J., Baillie, M.G.L., Bard, E., Bayliss, A., Beck, J.W., Bertrand, C., Blackwell, P.G., Buck, C.E., Burr, G., Cutler, K.B., Damon, P.E., Edwards, R.L., Fairbanks, R.G., Friedrich, M., Guilderson, T.P., Hughen, K.A., Kromer, B., McCormac, F.G., Manning, S., Bronk Ramsey, C., Reimer, R.W., Remmele, S., Southon, J.R., Stuiver, M., Talamo, S., Taylor, F.W., Van der Plicht, J., Weyhenmeyer, C.E., 2004. Radiocarbon 46, 1029–1058.
- Rice, D.S., 1976. Middle preclassic Maya settlement in the central Maya lowlands. *Journal of Field Archaeology* 3, 425–445.
- Rice, D.S., Rice, P.M., 1990. Population size and population change in the central Peten Lake region, Guatemala. In: Culbert, T.P., Rice, D.S. (Eds.), *Precolumbian Population History in the Maya Lowlands*. University of New Mexico Press, Albuquerque, pp. 123–148.
- Roubik, D.W., Moreno, J.E., 1991. Pollen and spores of Barro Colorado Island. *Miss Bot Garden* 36, 1–270.
- Russell, J.M., Talbot, M.R., Haskell, B.J., 2003. Mid-Holocene climate change in Lake Bosumtwi, Ghana. *Quaternary Research* 60, 133–141.
- Stott, L., Poulsen, C., Lund, S., Thunell, R., 2002. Super ENSO and global climate oscillations at millennial time scales. *Science* 297, 222–226.
- Timmermann, A., Krebs, U., Justino, F., Goosse, H., Ivanochko, T., 2005. Mechanisms for millennial-scale global synchronization during the last glacial period. *Paleoceanography* 20 (4), PA4008.
- Tedesco, K., Thunell, R., 2003. High resolution tropical climate record for the last 6000 years. *Geophysical Research Letters* 30, 1891, doi:10.1029/2003GL017959.
- Vaughan, H.H., Deevey, E.S., Garrett-Jones, S.E., 1985. Pollen stratigraphy of two cores from the Petén Lake district. In: Pohl, M.D. (Ed.), *Prehistoric Lowland Maya Environment and Subsistence Economy*. Papers of the Peabody Museum of Archaeology and Ethnology No. 77. Harvard University, Cambridge, pp. 73–89.
- Vinson, G.L., 1962. Upper Cretaceous and tertiary stratigraphy of Guatemala. *Bulletin of the American Association of Petroleum Geologists* 46, 425–456.
- Wahl, D., Byrne, R., Schreiner, T., Hansen, R., 2006. Holocene vegetation change in the northern Peten and its implications for Maya prehistory. *Quaternary Research* 65, 380–389.